Structural relaxation processes in poly(ethylene glycol) methacrylate macromonomers

1998 J. Phys.: Condens. Matter 10 545

(http://iopscience.iop.org/0953-8984/10/3/008)

J. Phys.: Condens. Matter **10** (1998) 545–556. Printed in the UK PII: S0953-8984(98)85123-0

Structural relaxation processes in poly(ethylene glycol) methacrylate macromonomers

F Aliotta, G Di Marco, M E Fontanella and M Lanza

Istituto di Tecniche Spettroscopiche del CNR, Salita Sperone 31, 98166 Messina, Italy

Received 17 June 1997, in final form 15 September 1997

Abstract. The investigation of the structural relaxation properties of poly(ethylene glycol) methacrylates are of practical interest, due to their ability to work as the inert backbone to which poly(ethylene oxide) oligomers can be attached to obtain highly amorphous polymeric matrices.

Two poly(ethylene glycol) methacrylate, PEGMA, macromonomers, with different side chain lengths, are investigated by the dielectric technique, in the frequency range 0.3–300 kHz, and by Brillouin scattering. The analysis of the Brillouin spectra gives evidence for the existence of a relaxation process in both the systems. Furthermore, a comparison of the normalized absorption data with their corresponding *classical* values (deduced from the shear viscosity data) suggests that what the Brillouin scattering experiment detects is a dissipative relaxational process in which the shear viscosity plays the main role. The comparison of the Brillouin scattering results with the dielectric data shows that what we are observing, in both the systems, is a single relaxation process. The temperature dependences of the relaxation times, observed on more than 10 decades, fail to follow simple Arrhenian behaviours. Both the systems can be interpreted as intermediate between *strong* and *fragile* liquids, following the Angell classification, and appear characterized by the existence of a wide variety of local structural environments, triggered by some relaxation process. Such a situation is more clearly evidenced by the macromonomer with longer chain. From the whole body of experimental data, it can be deduced that shorter-side-chain PEGMA macromonomers are better candidates for the formation of highly amorphous comb-branched polymers.

1. Introduction

Nowadays, a lot of know-how has been gained about techniques for the production of polymeric matrices with fixed properties. As a consequence, the engineering of a number of new materials and new devices, interesting both from the practical and the economic points of view, has become possible. As an example, we can recall polymeric electrolytes [1]: in these systems, a salt is solubilized within a suitable polymer that, in such a way, becomes able to assist the ionic diffusion. Conductibility values of the order of $10^{-5}\ \Omega^{-1}\ \mathrm{cm}^{-1}$ at room temperature are not unusual. Besides the main requirement that the adopted polymer works as a good solvent for the salt, one should take care in obtaining highly amorphous polymeric matrices (a high degree of disorder will promote the natural chain motions). Furthermore, the polymeric matrix should be characterized by a glass transition temperature much lower than the working temperature to enhance long-range cooperative motions.

Of course, interest is also focused on solubilizing other substances than salts. As an example, it became possible to make some gas sensors by dissolving a chromophore in a

0953-8984/98/030545+12$19.50

gas-permeable polymeric matrix [2–4]. If the luminescence of the system is influenced by the interaction of the solute with a specific gas dissolved in the atmosphere, one has just to monitor it: in such a way it is possible to carry out the building up of devices for the determination of the concentration of a given gas in the environment.

The ability of polyethylene oxide (PEO) to coordinate (through the unshared outer electronic pair of the oxygen) with a wide class of chemical species makes it one of the more promising and investigated systems. But, up to now, the adoption of PEO for practical devices has been limited due to its semicrystalline arrangement. In addition, an increase of T_g with the salt concentration is observed, that leads to the unwanted formation of further crystalline islands within its structure [5]. Summarizing, a good system should have the PEO ability to coordinate with different chemical species; at the same time, it should be highly amorphous. Crystallinity can be reduced by using short-chain-length poly(ethylene glycol) systems as the solvating medium, but such systems are not easy to handle due to their viscosity. The above difficulty can be overcome preparing comb-branched polymers with oligomeric PEO units attached to another polymer which acts as the inert backbone. The practical requirements seem to be fulfilled by poly(ethylene glycol) methacrylate (PEGMA, $H_2C{=}C(CH_3)CO(OCH_2CH_2)_nOH$) that is able to give rise, after polymerization, to comb-branched PEO copolymers [1].

In a previous experimental investigation [6] on mixed PEO–PEGMA systems, in which the macromonomer characterized by $n = 7$ was used, it was shown that, besides the ability to act as PEO plasticizer, PEGMA is able to lower the concentration of crystalline islands within the whole system.

In this paper we will try to gain new fundamental information about the structural relaxation processes in PEGMA. In particular, data from the macromonomer with $n = 7$ will be compared with data from the system with $n = 12$. In such a way some further indications are obtained about the role played by the PEGMA molecular weight on the degree of disorder in the obtained polymeric matrices and on the value of the glass transition temperature.

2. Experimental procedures and results

Samples of 2-hydroxyethyl methacrylate (HEMA, $H_2C{=}C(CH_3)CO(OCH_2CH_2)OH$) and poly(ethylene glycol) methacrylate (PEGMA) were purchased from Aldrich. The samples were put under vacuum to remove any unwanted gas and were used without further purification. In the following the samples with $n \sim 7$ and 12 will be referred to as PEGMA-a and PEGMA-b respectively.

Dielectric measurements were performed by a Rheometric Scientific analyser, in the temperature range $-130\,^{\circ}\mathrm{C} \leqslant T \leqslant -30\,^{\circ}\mathrm{C}$, with a rate of $1\,^{\circ}\mathrm{C\ min^{-1}}$. The analysis chamber was purged with nitrogen and the spanned frequencies were in the range 0.3 Hz–300 kHz.

The Brillouin scattering measurements were performed with a double-pass Fabry–Pérot interferometer (SOPRA). A cavity length was selected of about 6 mm, to which a free spectral range of 25 GHz corresponds. The true working free spectral range was determined by means of calibration with an H_2O sample at $T = 25\,^{\circ}\mathrm{C}$ and turned out to be 24.09 GHz. A value of 92 was obtained for the working finesse, determined by the experimental linewidth from a static scatterer (polystyrene colloidal suspension): in such a way the resolution was of about 130 MHz (half width at half maximum). The measurements were performed at different scattering angles in the range $30^{\circ} \leqslant \theta \leqslant 120^{\circ}$. Samples were placed in a

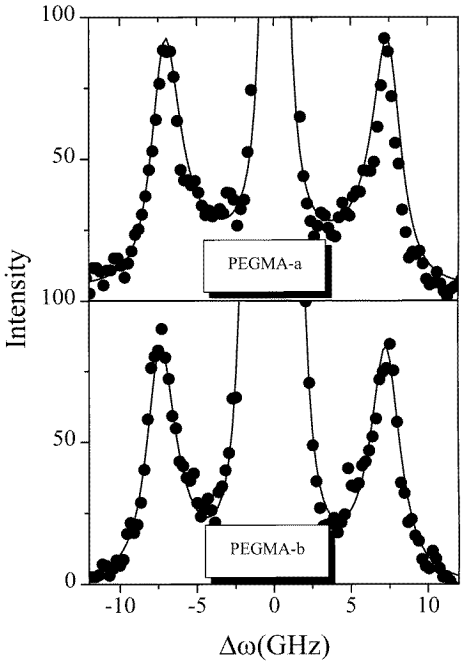

Figure 1. Brillouin spectra for PEGMA-a and PEGMA-b at $T = 25\,^{\circ}$C and $\theta = 90^{\circ}$. Continuous lines are the fitting results.

suitable home-made optical thermostat. The temperature was ranged from 9 to 44 °C with a stability accuracy better than 0.05 °C. The light source was a Spectra-Physics 171 Ar^{+} laser operating at 4880 Å. The mean power on the sample was about 300 mW through all the measurements.

In figure 1 we report, as an example, two experimental spectra for the samples PEGMA-a and PEGMA-b, obtained at $T = 22\,^{\circ}$C and at a scattering angle of 90°.

The profile of the scattering peaks reported in figure 1 is clearly asymmetric. As the temperature is increased the profile becomes more asymmetric while the peak position shifts toward lower frequencies. Such a result is a first direct evidence for some relaxational process taking place in the ps time scale. The experimental data were fitted according to the usual expression [7]:

$$I_{VV}(\omega) = \frac{A_R\Gamma_R}{\omega^2+\Gamma_R^2} + \left[\frac{A_B\Gamma_B}{[\omega-(\omega_B^2-\Gamma_B^2)^{1/2}]^2+\Gamma_B^2} + \frac{A_B\Gamma_B}{[\omega+(\omega_B^2-\Gamma_B^2)^{1/2}]^2+\Gamma_B^2}\right] + \frac{\Gamma_B}{\omega_B^2-\Gamma_B^2}\left[\frac{\omega-(\omega_B^2-\Gamma_B^2)^{1/2}}{[\omega-(\omega_B^2-\Gamma_B^2)^{1/2}]^2+\Gamma_B^2} + \frac{\omega+(\omega_B^2-\Gamma_B^2)^{1/2}}{[\omega+(\omega_B^2-\Gamma_B^2)^{1/2}]^2+\Gamma_B^2}\right] \quad (1)$$

where A_R and A_B are the intensities of the Rayleigh and Brillouin contributions respectively. In (1), the first term describes the quasi-elastic, resolution-enlarged central line, the next the symmetrical Brillouin contribution and the last the asymmetric contributions. The fitting procedure, whose results are reported as continuous lines in figure 1, furnishes the frequency shift ω_B and the HWHM Γ_B of the Brillouin lines. The values of the hypersonic velocity

and of the normalized absorption α/f^2 are then obtained according to the expressions:

$$v_h = \frac{\omega_B}{k}$$
$$\frac{\alpha}{f^2} = \frac{2\pi\Gamma_B}{v_h\omega_B^2} \tag{2}$$

with k the exchanged wave-vector.

In figures 2 and 3 the obtained frequency dependences of the hypersonic velocities at different temperatures are reported for the PEGMA-a and PEGMA-b samples.

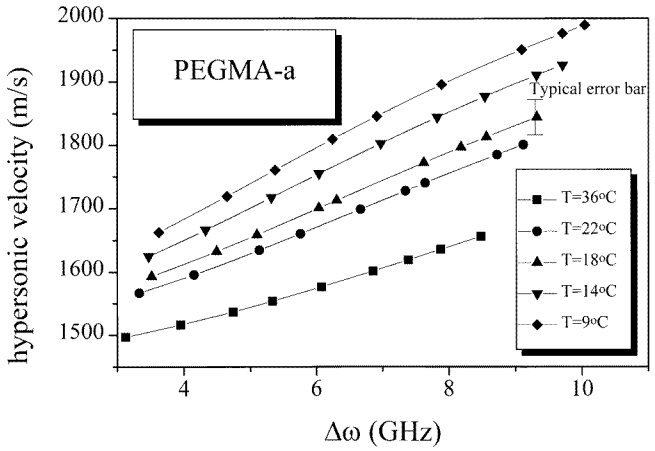

Figure 2. Frequency dependence of the hypersonic velocity at different temperatures for PEGMA-a. Continuous lines are the fitting results.

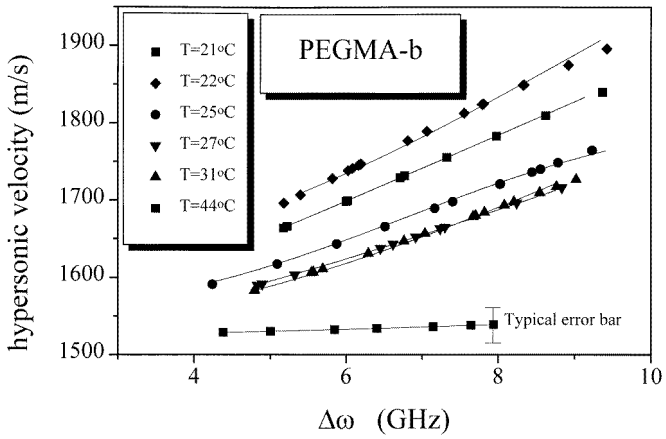

Figure 3. Frequency dependence of the hypersonic velocity at different temperatures for PEGMA-b. Continuous lines are the fitting results.

Complementary measurements of ultrasonic velocity have been performed by means of a standard MATEC pulse-echo analyser. Data were collected at 3, 9 and 15 MHz, as a

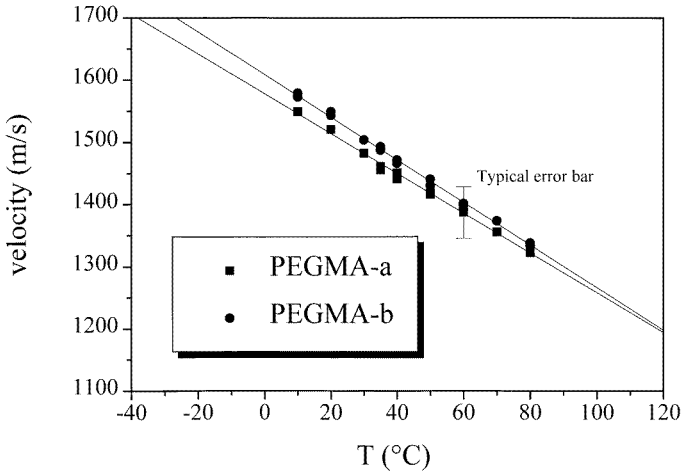

Figure 4. Ultrasonic velocity data for PEGMA-a and PEGMA-b.

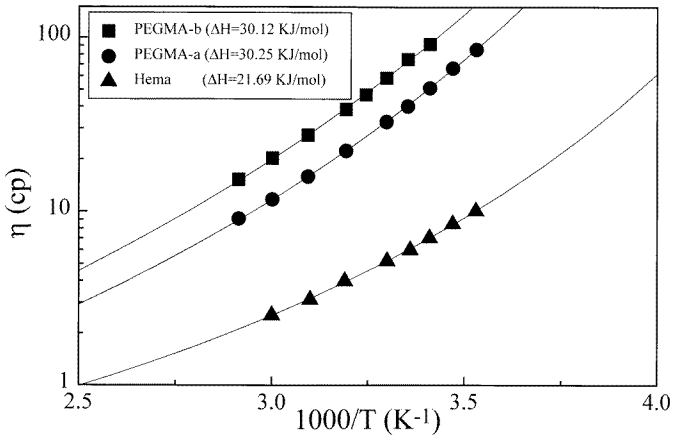

Figure 5. Vogel–Fulcher–Tamman behaviour of the viscosity data for HEMA, PEGMA-a and PEGMA-b.

function of the temperature in the range $10\,^{\circ}\mathrm{C} \leqslant T \leqslant 80\,^{\circ}\mathrm{C}$. For both the samples the data turned out to be frequency independent, at least in the explored range. Such an occurrence makes us confident in assuming the obtained sound velocity as v_0. The obtained temperature dependences for the ultrasonic velocities are reported in figure 4.

Furthermore, viscosity measurements were performed on HEMA as well as on the PEGMA samples. The measurements were performed by means of a series of Ubbelohde viscometers of different shear rates. Care was taken in changing them until the measured viscosity became independent of the shear rate. In such a way, taking into account the sound velocity data giving an indication of a relaxation process centred at higher frequency, we can assume that the resulting data represent η_0. The shear viscosity data are reported in figure 5.

3. Analysis of the data and discussions

The hypothesis of a relaxation process is confirmed by the presence of an inflexion point at about 5–6 GHz in the frequency behaviour of the hypersound velocity both in PEGMA-a and in PEGMA-b.

If one remembers that what we are observing is a spontaneous scattering phenomenon in a moderately viscous fluid, it is possible to assume the validity of the linear viscoelastic theory on which basis we can derive some expressions for the complex longitudinal modulus [7], $\tilde{M}$, whose real part, M' (the storage modulus), is connected with the sound speed while its imaginary part, M'' (the loss modulus), is related to the sound absorption. Generally, in associated liquids the relaxation processes take place with an appropriate distribution function $f(\tau)$ and the complex longitudinal modulus can be written as:

$$\tilde{M} = \tilde{M}_0 - (\tilde{M}_\infty - \tilde{M}_0) \int_{-\infty}^{+\infty} f(\tau) \frac{\mathrm{i}\omega\tau}{1 - \mathrm{i}\omega\tau} \, \mathrm{d}\tau. \tag{3}$$

If n separate relaxation events occur in the system, the integral in (3) is substituted by a sum over n steps. A more simplified assumption is that the relaxation processes are well decoupled into separate steps and that, for each step, the distribution $f(\tau)$ is *narrow*: in such a way, the relaxation time of each step can be considered as a mean value. Under this assumption (that in our case can be a workable assumption, because we are far from the glass transition and the temperature dependence of the relaxation parameters is not too far from the Arrhenian behaviour) the equation (3) can be written as:

$$\tilde{M} = M' + \mathrm{i}M'' = K_r^{str} \frac{\omega^2\tau_v^2}{1 + \omega^2\tau_v^2} + \mathrm{i}\omega\eta_v(\omega) + \frac{4}{3} G_\infty \frac{\omega^2\tau_s^2}{1 + \omega^2\tau_s^2} + \mathrm{i}\frac{4}{3}\omega\eta_s(\omega). \tag{4}$$

In the above equation, K_r^{str} is the relaxing compressional modulus, G_∞ is the high-frequency value of the shear modulus (or rigidity modulus) and τ_v and τ_s are respectively the structural and the shear relaxation times. It should be stressed that the high-frequency normalized absorption data are definitely lower than their *classical* (or Stokes) values, $(\alpha/f^2)_{cl} = (2\pi^2/\rho_0 v_0^2)(\frac{4}{3}\eta_s)$ (with ρ_0 the macroscopic density), and that the difference between the two sets of data increases when the temperature is lowered (see table 1, where the hypersonic absorption values from data obtained at a scattering angle $\theta = 90^\circ$ are compared with the corresponding classical values). Such a result assures us that we are in the presence of a dissipative relaxational process in which the shear viscosity plays the main role. Following such a consideration we have assumed a single-shear-relaxation model:

$$\tilde{M} = \tilde{M}_0 = G' + \mathrm{i}G'' = \frac{4}{3} G_\infty \frac{\omega^2\tau_s^2}{1 + \omega^2\tau_s^2} + \mathrm{i}\omega\frac{4}{3} G_\infty \frac{\tau_s}{1 + \omega^2\tau_s^2} \tag{5}$$

according to which our hypersonic velocity and absorption data can be fitted to the equations:

$$v_h^2(\omega, T) = \frac{1}{\rho_0(T)} \left[\rho_0(T) v_0^2(T) + \frac{4}{3} G_\infty(T) \frac{\omega^2\tau_s^2(T)}{1 + \omega^2\tau_s^2(T)} \right] \tag{6}$$

$$\frac{\alpha(\omega, T)}{f^2} = \frac{2\pi^2}{\rho_0(T) v_s^3} \left[\frac{4}{3} G_\infty(T) \frac{\tau_s^2(T)}{1 + \omega^2\tau_s^2(T)} \right] + \text{constant}. \tag{7}$$

In the above expressions, the symbols have the usual meaning, $v_0(T)$ corresponds to the low-frequency value of the sound velocity, as obtained by ultrasonic measurements, and the constant term in the expression for the normalized absorption takes into account all the high-frequency non-relaxing contributions.

Table 1. Temperature dependence of the normalized hypersonic absorption, α/f^2, classical absorption, $(\alpha/f^2)_{cl}$, and shear viscosity, η_s.

Sample	T (°C)	$\frac{\alpha}{f^2} \times 10^{14}$ s^2 m^{-1}	$\left(\frac{\alpha}{f^2}\right)_{cl} \times 10^{14}$ s^2 m^{-1}	$\eta_s \times 10^2$ poise
PEGMA-a	9	13 ± 4	43 ± 2	85.4 ± 0.1
	14	13 ± 4	36 ± 2	66.6 ± 0.1
	18	16 ± 5	29 ± 1	51.2 ± 0.1
	22	14 ± 4	24 ± 1	40.2 ± 0.1
	36	18 ± 5	16 ± 1	22.5 ± 0.1
PEGMA-b	21	6 ± 2	52 ± 3	91.8 ± 0.1
	25	6 ± 2	47 ± 2	80.0 ± 0.1
	27	6 ± 2	37 ± 2	59.0 ± 0.1
	31	7 ± 2	38 ± 2	58.5 ± 0.1
	44	6 ± 2	21 ± 1	28.0 ± 0.1

Table 2. Relaxation time fitted with Vogel–Fulcher–Tamman or Arrhenius laws.

Sample	VFT D	VFT T_0 (K)	Arrhenius ΔH_{die} (kJ mol^{-1})	Arrhenius ΔH_{hyp} (kJ mol^{-1})
PEGMA-a	8.65	147.3	171.53	13.78
PEGMA-b	8.65	146.5	164.88	20.70

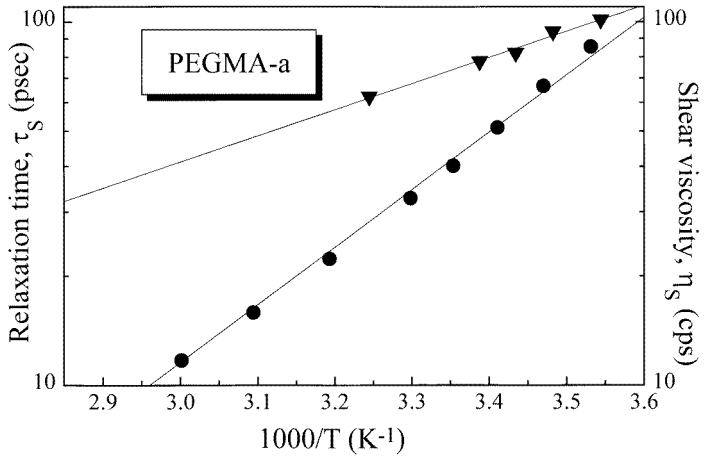

Figure 6. Arrhenius plot of the shear viscosity (triangles) and relaxation time (circles) for PEGMA-a.

The continuous lines reported in the figures 2 and 3 represent the results from the fitting procedure of the hypersonic velocity data with the above equation and the low-frequency values taken from figure 4.

In the figures 6 and 7, we report in Arrhenius plots the obtained relaxation times for the two samples, together with the corresponding behaviours for the shear viscosity.

In both samples the activation energy for the viscous flow (considered as a mean value in the explored temperature range) is definitely higher than that for the shear relaxation

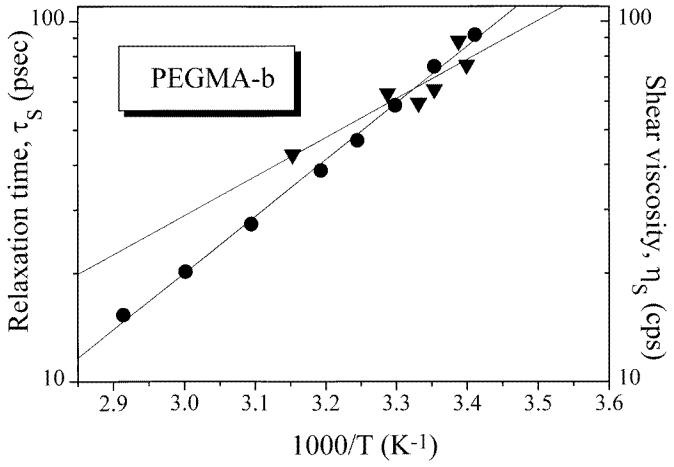

Figure 7. Arrhenius plot of the shear viscosity (triangles) and relaxation time (circles) for PEGMA-b.

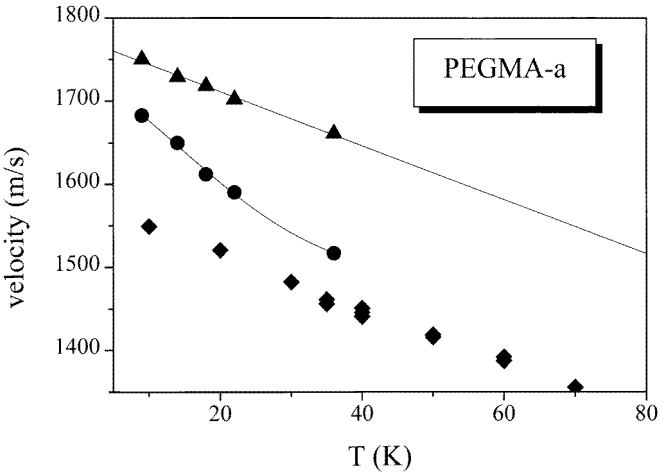

Figure 8. Temperature evolution of the hypersonic velocity for PEGMA-a (circles). Rhombuses represent ultrasonic data while triangles are calculated v_∞ data.

time, suggesting the idea that a distribution of relaxation processes is taking place in both systems (see table 2).

The situation is well depicted in figures 8 and 9, where the temperature dependences of the hypersonic velocities are reported, for both the samples, at a frequency of 4 GHz. In the same figures are reported the v_0 data, obtained by ultrasonic measurements, and the calculated high-frequency limit velocity. Both the samples show, at the investigated frequency and within the spanned temperature range, a transition from a purely dissipative viscous system to an elastic pseudoglass [8].

The challenge is concerned with finding a description of the detected relaxation process that is consistent with other relaxing behaviours detected by other techniques at lower frequencies. As a matter of fact, we can assert that the relaxational behaviour in polymers

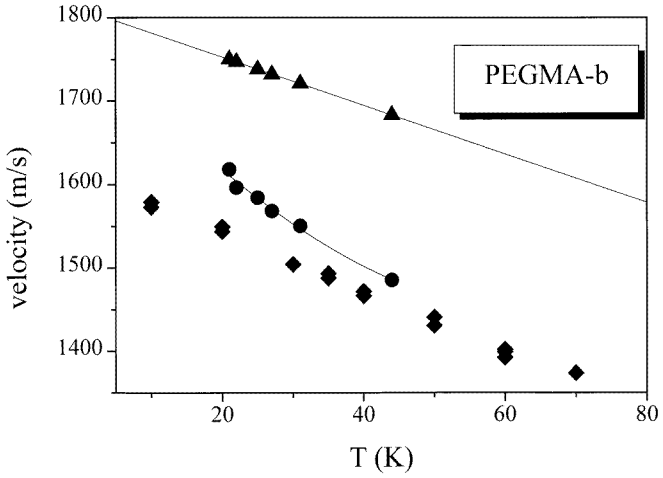

Figure 9. Temperature evolution of the hypersonic velocity for PEGMA-b (circles). Rhombuses represent ultrasonic data while triangles are calculated v_∞ data.

appears to follow a quite universal picture: at a cross-over temperature, T_c, located above the glass transition temperature, T_g, there is a splitting from a high-temperature regime with a single relaxation time to two separate low-frequency processes. It is customary to distinguish a slow structural process, α relaxation, and a fast, β, relaxation. Usually, the α relaxation is attributed to intermolecular interactions of several monomers originated by micro-Brownian motions (glass transition) while the β relaxation is described in terms of side-group or end-group rotations [9, 10]. On the other hand, in some systems, described as *fragile* liquids following the Angell classification [11, 12], the bifurcation between the two relaxational processes has been attributed to decoupling between diffusion and vibration [13]. The systems under investigation appear more similar to *fragile liquids*, with evidence of only one relaxation process cooperative in character. Such a finding should not be surprising if one takes into account the very short chain lengths. The relaxation time, τ, associated with the detected cooperative relaxation, is well described by a Vogel–Fulcher–Tamman equation:

$$\tau = \tau_0 \exp \frac{DT_0}{T - T_0} \tag{8}$$

with t_0 the relaxation time in the high-temperature limit and T_0 the temperature where τ diverges. The different behaviours as a function of the temperature evidenced by one system or another are essentially determined by the value of the parameter D. The meaning of D can be understood if one remembers the suggestion of Gibbs [14] that, when the shear relaxation is fully coupled to structure, the relaxation time, τ_s, is governed by the state of liquid disorder represented by the configurational entropy, S_C, and is a function of the height of energy barrier, $\Delta\mu$, over which the cooperatively rearranging group [15] must pass. Taking into account that any experimental failure of the Arrhenius law should be the consequence of a temperature dependence of the configurational entropy and after the adoption of a suitable form for the temperature dependence of the heat capacity (on which S_C depends), Angell and Sichina [16] were able to derive the Vogel–Fulcher–Tamman expression. Following such an approach it can immediately be realized that the parameter D in (7) contains two contributions, one thermodynamic in character and the other kinetic.

An indication towards the description of our systems in terms of *fragile* liquids and, as a consequence, towards the description of the observed phenomenon in terms of a distribution of relaxational processes is given by the occurrence that the viscosity data, reported in figure 5, fail to follow exactly a simple Arrhenian behaviour and are well fitted in agreement with a Vogel–Fulcher–Tamman law (see table 3).

Table 3. Viscosity data fitted with Vogel–Fulcher–Tamman or Arrhenius laws.

Sample	VFT D	VFT T_0 (K)	Arrhenius ΔH_η (kJ mol^{-1})
HEMA	3.43	163.1	21.69
PEGMA-a	5.75	156.1	30.25
PEGMA-b	6.99	147.9	30.12

In particular, the values for the D parameter reported in table 3 seem to indicate an increasingly *fragile* character with increasing molecular weight.

In figure 10 the relaxation times obtained by the analysis of the Brillouin data for the two samples are reported, together with the results for the relaxation obtained by low-frequency dielectric measurements. In figure 11 we report, as an example, the behaviour of $\tan\delta$ (dielectric measurements) at three different frequencies for the two samples. A relaxational peak is clearly evident for both the PEGMA samples. The main difference between the behaviours reported in figure 11(a) and (b) is the occurrence that the relaxational process appears to take place at higher temperature for the larger molecule. The comparison of the dielectric data with the hypersonic relaxation times (see figure 10) would suggest that we are observing an α relaxation. Such an indication is given by the occurrence that the behaviour is clearly non-Arrhenian, when observed on a wide enough frequency range. The hypothesis is in agreement with the collective character of the hyperacoustic relaxation reported in figures 8 and 9. Furthermore, the data reported in figure 11 would suggest that relaxation phenomena observed in the two systems are interpretable as originating from the same cooperative structural rearrangement.

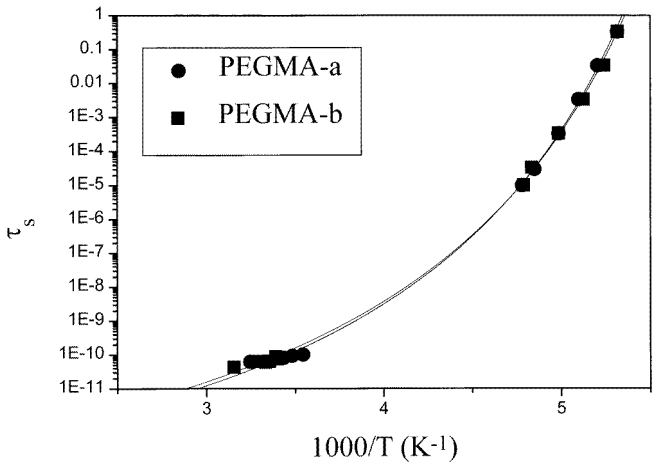

Figure 10. Temperature dependence of the relaxation times for PEGMA-a and PEGMA-b.

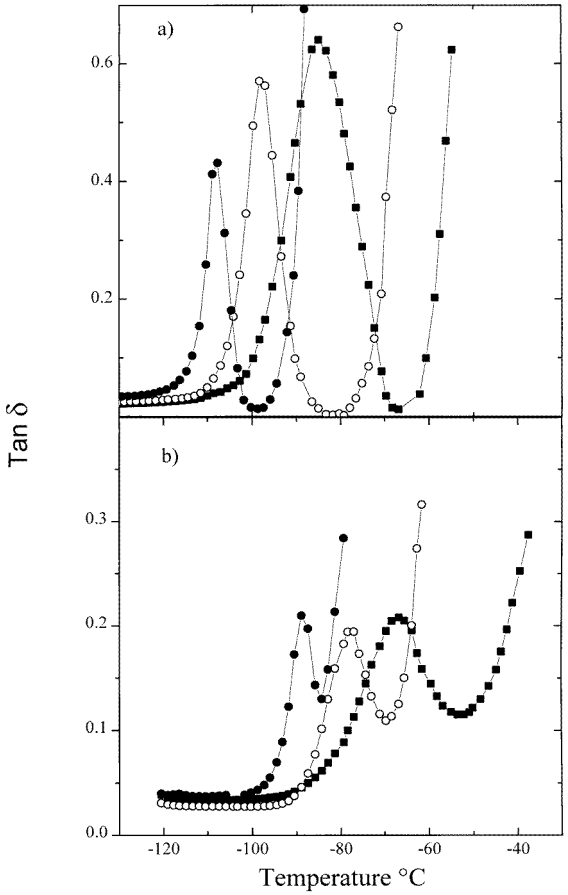

Figure 11. Dielectric response for (a) PEGMA-a and (b) PEGMA-b as a function of the temperature. Solid circles: 0.3 Hz. Open circles: 300 Hz. Squares: 30 kHz.

The plots reported in figure 10 allow us to follow the temperature dependence of the relaxation time over more than 10 decades. The Vogel–Fulcher–Tamman fit of the data reported in figure 10 furnishes evidence for a more fragile character of the two systems than that estimated by the shear viscosity data only (see table 2).

Really, if one looks accurately at the data reported in figure 10, it is possible to observe that, while the average value of the relaxation times, deduced by the Brillouin experiment, agrees with the VFT extrapolation of the low-frequency data, the slopes of the high-frequency Arrhenius fits (reported in figures 6 and 7) diverge from that of the VFT curve (in effect the VFT result represented in figure 10 is not too far from the VFT behaviour evidenced by the shear viscosity, as can be easily confirmed by a comparison between the data reported in table 2 and in table 3).

The above-mentioned discrepancy is, up to now, not elucidated. At the moment we can only hypothesize that what we are observing in the Brillouin scattering experiment is a structural relaxation coupled or disturbed by the local motions of the structural units.

Furthermore, our data seem to indicate that such a disturbance is more efficient in longer chains (compare figure 6 with figure 7).

4. Concluding remarks

In summary, the whole body of the experimental data, indicating a VFT behaviour of the low-frequency relaxation together with an Arrhenian or near-Arrhenian temperature dependence of the relaxational process probed by Brillouin scattering, suggests classifying our systems as intermediate between strong (Arrhenian-like) and fragile (non-Arrhenian-like) liquids. If one recalls the Angell description in terms of the density of minima in the potential energy hypersurface in the $(3N + 1)$-dimensional configuration space of the N-particle molecular system [17], the above-presented data seem to depict our systems as characterized by a potential hypersurface on which a high density of minima exists with exceptionally high values of the free energy barriers between them. The high density of minima should correspond to a large variety of local structural environments triggered by some local relaxation. Such a situation is more clearly evidenced in the system with higher average molecular weight. Such a description would suggest considering our system as fragile from the thermodynamic point of view but, at the same time, kinetically strong (please remember the meaning of the D parameter).

The more fragile character evidenced by the PEGMA macromonomer with higher molecular weight would suggest that the smaller macromonomer should be a better candidate for the formation of highly amorphous comb-branched systems. The same indication comes from the lower value of the glass transition temperature evidenced by PEGMA-a with respect to PEGMA-b.

The result agrees with previous experimental results, obtained by Xia and coworkers on branched 2-methoxyethyl poly(ethylene glycol) methacrylates [18, 19], showing the tendency, for high-molecular-weight macromonomers, to develop side chain crystallinity.

References

[1] MacCallum J R and Vincent C A (eds) 1987 *Polymer Electrolyte Reviews* vol 1 (London: Elsevier)
[2] Di Marco G, Lanza M and Campagna S 1995 *Adv. Mater.* **7** 468
[3] Di Marco G, Lanza M, Pieruccini M and Campagna S 1996 *Adv. Mater.* **8** 576
[4] Demas J N and De Graff M A 1991 *Anal. Chem.* **63** 829A
[5] Lee Y L and Crist B 1986 *J. Appl. Phys.* **60** 2683
[6] Di Marco G, Lanza M and Pieruccini M 1996 *Solid State Ion.* **89** 117
[7] Boon J P and Yip S 1980 *Molecular Hydrodynamics* (New York: McGraw-Hill) and references therein
[8] Litovitz T A and Davis C M 1965 *Physical Acoustic* vol 2, part A, ed W P Mason (New York: Academic) ch 5
[9] Murthy S S N, Sobhanadri J and Gangasharan J 1994 *J. Chem. Phys.* **100** 4601
[10] Wu L 1992 *Phys. Rev.* B **43** 9906
[11] Angell C A 1988 *J. Phys. Solids* **49** 863
[12] Angell C A 1991 *Hydrogen-Bonded Liquids* ed J C Dore and J Texeira (Deventer: Kluwer) pp 59–79
[13] Jäckle J 1986 *Rep. Prog. Phys.* **49** 171
[14] Gibbs J H 1960 *Modern Aspects of the Vitreous State* (London: Butterworth)
[15] Adam G and Gibbs J H 1965 *J. Chem. Phys.* **43** 139
[16] Angell C A and Sichina W 1976 *Ann. NY Acad. Sci.* **279** 53
[17] Angell C A 1988 *J. Phys. Chem. Solids* **49** 863
[18] Xia D W, Soltz D and Smidt J 1984 *Solid State Ion.* **14** 221
[19] Xia D W and Smidt J 1984 *J. Polym. Sci. Polym. Lett. Edn.* **22** 617